Effective beam pattern of the Blainville's beaked whale (*Mesoplodon densirostris*) and implications for passive acoustic monitoring

Jessica Ward Shaffer,[a] David Moretti, and Susan Jarvis
Naval Undersea Warfare Center Division Newport, Code 74, 1176 Howell Street, Newport, Rhode Island 02841-1708

Peter Tyack and Mark Johnson
Sea Mammal Research Unit, University of St. Andrews, Fife KY16 8LB, United Kingdom

(Received 1 June 2012; revised 16 December 2012; accepted 21 December 2012)

The presence of beaked whales in mass-strandings coincident with navy maneuvers has prompted the development of methods to detect these cryptic animals. Blainville's beaked whales, *Mesoplodon densirostris*, produce distinctive echolocation clicks during long foraging dives making passive acoustic detection a possibility. However, performance of passive acoustic monitoring depends upon the source level, beam pattern, and clicking behavior of the whales. In this study, clicks recorded from Digital acoustic Tags (DTags) attached to four *M. densirostris* were linked to simultaneous recordings from an 82-hydrophone bottom-mounted array to derive the source level and beam pattern of the clicks, as steps towards estimating their detectability. The mean estimated on-axis apparent source level for the four whales was 201 dB_{rms97}. The mean 3 dB beamwidth and directivity index, estimated from sequences of clicks directed towards the far-field hydrophones, were 13° and 23 dB, respectively. While searching for prey, Blainville's beaked whales scan their heads horizontally at a mean rate of 3.6°/s over an angular range of some +/−10°. Thus, while the DI indicates a narrow beam, the area of ensonification over a complete foraging dive is large given the combined effects of body and head movements associated with foraging.
[http://dx.doi.org/10.1121/1.4776177]

PACS number(s): 43.80.Ka, 43.30.Wi [AMT] Pages: 1770–1784

I. INTRODUCTION

Within the last decade, the sensitivity of some species of beaked whales (Cetacea: Odontoceti: Ziphiidae) to naval sonar has been well documented (Tyack *et al.*, 2011; D'Amico *et al.*, 2009), creating a need for effective monitoring in regions where their presence overlaps with navy sonar use. One of the sensitive species, Blainville's beaked whale (*Mesoplodon densirostris*), dives to great depths to forage, spending only a short period of time at the surface, resulting in a low probability of visual detection (Tyack *et al.*, 2006; Barlow, 1999). During deep foraging dives, *M. densirostris* produce distinctive echolocation clicks at a relatively steady rate while searching for prey, making them a candidate for passive acoustic monitoring (PAM) (Tyack *et al.*, 2006).

Much of what is known about the foraging behavior and sound production of this species has come from sound and movement recording tags attached to the dorsal surface of animals (Johnson and Tyack, 2003; Madsen *et al.*, 2005; Zimmer *et al.*, 2005). Similar data have also been obtained from Cuvier's beaked whale (*Ziphius cavirostris*), another species considered to be sensitive to sonar (D'Amico *et al.*, 2009). These data have been used to design PAM systems (Mellinger *et al.*, 2007) and to predict the detection rate of beaked whales as a function of sound propagation conditions and ambient noise level (Zimmer *et al.*, 2008). Sounds recorded by a tag attached to an animal cannot be used to deduce the far-field on-axis characteristics of directional sounds such as echolocation clicks since the tag is located behind the sound source and so far off the acoustic axis (Johnson *et al.*, 2009). To overcome this problem, sound source characteristics have been gleaned from clicks recorded from other animals near the tagged animal but the unknown distance and orientation of the clicking animal limits the potential to estimate source level and beam pattern (Johnson *et al.*, 2006). Although the situation improves when multiple animals are tagged in a group (Zimmer *et al.*, 2005), this is seldom achieved in practice. Thus, although rough source level and beam width estimates have been made for *M. densirostris* (source level only, Johnson *et al.*, 2004) and *Z. cavirostris* (Zimmer *et al.*, 2005), more accurate information is lacking. This information is critically important as the objective of PAM is extended beyond presence/absence monitoring to more complex tasks such as density estimation (Marques *et al.*, 2009), population health, and group dynamics.

Beaked whales have long been sighted at the U.S. Navy's undersea range in the Tongue of the Ocean (TOTO), Bahamas, but were not acoustically detected and recorded until 2004, when the recording bandwidth for marine mammal monitoring was increased (DiMarzio *et al.*, 2008). In 2005, visual confirmation of the species by trained observers (D. Claridge, personal communication) in tandem with

[a]Author to whom correspondence should be addressed. Electronic mail: jessica.a.shaffer@navy.mil

recordings on the Atlantic Undersea Test and Evaluation Center (AUTEC) bottom mounted hydrophone array provided some of the first far-field sound recordings of *M. densirostris*. Towed and moored hydrophone arrays have since been used to describe the sounds made by other beaked whale species avoiding the difficulties associated with applying tags to these cryptic species. Visually confirmed towed array recordings of *M. europaeus*, a species also present in Bahamian waters, and *Hyperoodon ampulatus* have been reported to have similar characteristics to *M. densirostris* and *Z. cavirostris* clicks (Gillespie *et al.*, 2009; Wahlberg *et al.*, 2011) but with slightly different center frequencies. Autonomous recorders have recorded beaked whale-like sounds in a variety of areas (Baumann-Pickering *et al.*, 2010) over long durations, although it has proven challenging to allocate these sounds to species in the absence of visual confirmation.

Taken together, tag studies and far-field recordings suggest that several species of beaked whales produce clicks that can reliably be identified for long intervals during foraging dives. The dive cycle of *M. densirostris* has a mean length of 140 min, comprising a roughly 45 min deep foraging dive to depths of up to 1250 m followed by a sequence of short resting dives at the surface (Tyack *et al.*, 2006). This species is silent during much of the descent and ascent from foraging dives as well as during shallow dives. During deep foraging dives, *M. densirostris* produce two types of clicks: regular foraging clicks with a mean interclick interval (ICI) of 0.37 s and buzz clicks that occur in short bursts with a mean duration of 2.9 s (Johnson *et al.*, 2006). Regular clicks consist of an FM upsweep with a −10 dB bandwidth of 26 to 51 kHz and a median duration of 271 μs (Johnson *et al.*, 2006). Overall *M. densirostris* produce sequences of clicks for 18% of the time (Aguilar de Soto *et al.*, 2011). Echoes from prey recorded by a tag have been used to deduce a source level for FM clicks in the range of 200–220 $dB_{peak\text{-}to\text{-}peak\ (pp)}$ re 1 μPa at 1 m (Johnson *et al.*, 2004).

The effectiveness of a passive acoustic monitoring system is measured by its probability of detection (P_d) for a given probability of false alarm (P_{fa}). Depending on the application, the event to be detected (and therefore the P_d) may refer to a single click, to a foraging dive made by an individual animal, or to synchronized dives by a group of animals. The resulting P_d depends on the number of hydrophones in the receiver, their spatial distribution and the way the signals from these are processed, as well as on the behavior of the animals and the acoustic characteristics of the environment. Although PAM systems with a single hydrophone are effective at detecting animals, an array of multiple hydrophones, such as that at AUTEC, provide the possibility of localizing individuals or groups of animals (DiMarzio *et al.*, 2008; Ward *et al.*, 2008), which may be critical for mitigation or abundance estimation. The species-specific transmission beam pattern influences the facility with which animals can be localized by a hydrophone array (Wahlberg *et al.*, 2011). Localization requires that clicks are detected on multiple spatially separated hydrophones but this is unlikely to occur in a large aperture hydrophone array such as at AUTEC if the click beam pattern is narrow. Conversely, if the array aperture is small enough that all of the hydrophones are within a narrow click beam, the localization accuracy of the system will be limited. For example, an autonomous small aperture (0.5 m) four hydrophone tetrahedral array was able to track beaked whales within an 800 m range (Wiggins *et al.*, 2012) but, while the angle-of-arrival accuracy may be high, ranging errors will increase substantially with range.

The directionality of a sound source is parameterized by its directivity index (DI): the larger the DI, the more directional the beam (Au, 1993) and the more difficult it will be to localize the source. Directionality also impacts P_d because, even though a narrow beam will be detectable at a greater range on axis, the probability that the beam will ensonify a far-field hydrophone is lower. However, P_d is, in general, a complex function of the source level, spectrum and duration of clicks, making joint knowledge of these parameters important for the design of effective PAM systems.

Estimation of the beam pattern requires hydrophone measurements in the far-field of the animal at a variety of angles with respect to the acoustic axis. Both the range of the animal to the hydrophone and the relative orientation of its acoustic axis are required for each sound recorded. Measurements of captive odontocetes have shown that several source parameters change as a function of increasing off-axis angle, with the source level and center frequency decreasing, and click duration increasing (Au, 1993). These measurements are often made in a controlled tank environment with trained animals either using a stationary bite plate with sensors placed on the head (Au, 1993) or a small hydrophone array with a video camera to determine when animals are swimming directly toward the array (Au *et al.*, 1999). In both cases, the array is either placed directly in front of, or within several meters of, the animal. For animals not available in captivity, beam pattern is considerably more difficult to measure. Rasmussen *et al.* (2004) used a co-located camera and hydrophone array to estimate the beam pattern of white-beaked dolphins (*Lagenorhynchus albirostris*), but this requires close approaches of vocalizing animals. For larger free-ranging odontocetes, the distance can be calculated from the arrival times of sounds at a hydrophone array (Wahlberg *et al.*, 2011), but animals are often beyond the operating range of cameras, and so the orientation of the vocalizing whale must also be deduced from the received signals. Nosal and Frazer (2007) used sound arrival times at the AUTEC hydrophone array to estimate position, swim velocity and thereby orientation and beam pattern of vocalizing sperm whales, but this differential method requires highly precise localizations. An alternative approach, described by Zimmer *et al.* (2003), is to make far-field array recordings of animals tagged with a sound and movement recording tag such as the DTAG (Johnson and Tyack, 2003). The orientation of the animal at the time of each click can be deduced from the sensors in the tag and combined with the received level at the far-field hydrophone to infer the beam pattern. A key requirement in this approach is that of locating the animal accurately with respect to the receiving array. Zimmer *et al.* (2003) used a linear towed array to estimate the range and bearing to a tagged sperm whale but the positional

accuracy of this approach declines rapidly with range, requiring long arrays and careful maneuvering to stay close to animals. While this may be achievable with sperm whales that click about 70% of the time (Watwood *et al*., 2006), the long non-vocal intervals of beaked whales make close follows impractical.

Here the method of Zimmer *et al*. (2003) is adapted for use with a unique PAM resource: the 82 hydrophone bottom-mounted array at AUTEC. The large aperture and spatial coverage of this array enables continuous accurate tracking of tagged animals, opening the way for measurements of source level and beam pattern. However, the improved localization accuracy highlights several other sources of error that must be considered both in estimating the transmission beam pattern and in modeling PAM performance. Even with the body orientation known precisely from a tag, the orientation of the head, and therefore the sound source, may differ from the body orientation as the animal moves its head independently of body motions while echolocating (Rasmussen *et al*., 2004; Zimmer *et al*., 2005). This leads to an apparent widening of the beam pattern when averaged over multiple clicks that may increase the probability of detection of a PAM system. The actual source level may also vary from click to click as the animal clicks with greater or lesser effort leading to another difference between the instantaneous and average characteristics of the sound source (Madsen *et al*., 2005). Here we combine tag and far-field data to quantify these variations. The angle of arrival of sounds from the tagged animal at a stereo recording tag gives an indication of head turning while the relative level of clicks received at the tag provides an estimate of source level variation across multiple scans.

Here, sound recordings from the AUTEC hydrophone array are used to estimate the acoustic transmission characteristics of four tagged *M. densirostris*. The distribution of several parameters that are needed to evaluate the performance of a PAM system are presented, including body orientation, vocalization duration, head movement, inter-click interval (ICI), and variation in apparent output level (AO). The estimated source level (SL) as a function of orientation of the whale's acoustic axis with respect to the bottom-mounted hydrophones provides an estimate of the transmission beam pattern. The influence of these parameters on the probability of detecting beaked whales acoustically is discussed. The sound transmission characteristics of these four *M. densirostris* are then compared with the objective of determining if there are individually identifiable characteristics that might aid abundance estimation of foraging groups of beaked whales.

II. METHODS

Four *M. densirostris* were tagged with DTAG sound and movement recording tags in the Tongue of the Ocean, Bahamas, during the 2006 Species Verification Test and the 2007 Behavioral Response Study (Boyd *et al*., 2007). Calls made by the tagged animals were recorded simultaneously at an array of bottom mounted hydrophones. Tagged whales were photographed for individual identification, and then followed from a distance to identify the size and composition of the social group with which they were associated.

A. DTag data

Accelerometer, magnetometer, and pressure sensors in the tag were sampled at 50 Hz. The measurements were processed using the methods described in Johnson and Tyack (2003), resulting in heading, pitch, roll, and depth data sampled at 5 Hz. The depth measurement is within 5% of the true value. Orientation precision is better than 1° and absolute accuracy is approximately +/−3°. The DTag recorded audio at a 192 kHz sampling rate (400 Hz to 80 kHz bandwidth) from two front-mounted hydrophones separated horizontally by 2.5 cm. Clicks from the tagged whale were differentiated from those of nearby conspecifics by spectral cues and angle of arrival at the tag (Johnson *et al*., 2006). The time-of-emission (TOE) of each click relative to the tag clock was measured along with the horizontal angle of arrival (AoA) calculated as $\sin^{-1}(\tau c/d)$ where τ is the time delay between hydrophones receiving the click, c is the speed of sound in seawater, and d is the 2.5 cm distance between hydrophones (Johnson *et al*., 2006). The apparent output (AO, i.e., the sound level of the near-field off-axis signal recorded by the tag) for each click produced by the tagged whale was also determined.

B. Hydrophone click detection and localization

The tagged whales were synchronously recorded by AUTEC's 82 hydrophone wide-baseline array located on the seafloor of the TOTO. The hydrophones are mounted 4–5 m off the sea floor and have an upward, frequency-dependent, roughly hemispherical, beam pattern (Maripro Incorporated, 2002). The beam pattern becomes increasingly less sensitive in the direction of the water surface at the higher frequencies of *M. densirostris* vocalizations (e.g., greater than 24 kHz) (Maripro Incorporated, 2002). The recordings were made using multiple Alesis HD24 digital 24-bit recorders sampled at 96 kHz, which resulted in a usable frequency range from 50 Hz to approximately 48 kHz. Each Alesis HD24 can record up to 12 sound channels with one channel assigned to record an IRIG-B modulated time signal code. The IRIG-B amplitude-modulated signal is based on a sine wave carrier with a frequency of 1 kHz that contains time-of-year and year information, as well as seconds-of-day, with a once per second update rate.

To monitor the study area in real-time, the hydrophone array data were processed using a Fast Fourier Transform (FFT) based energy detector and frequency band classifier. The detector performs a 2048 point FFT with 50% overlap resulting in a frequency resolution of 47 Hz per bin and a 10.7 ms time step per bin. The magnitude of each bin of the FFT was calculated and then compared to a noise-varying threshold for that bin (Ward *et al*., 2008). The resulting detection spectrum was a binary representation of detection (1) or no detection (0) information per bin. If any of the bins passed the threshold, the binary FFT result was archived to file. The frequency band classifier then compared the ratio of frequency bins detected above 24 kHz, i.e., within the

beaked whale vocalization range, to those below 24 kHz. If at least 10 bins were detected above 24 kHz and the high frequency content was greater than 50% of detected bins, the detection was retained as a possible beaked whale click.

The click TOEs from the DTag were correlated using cross correlation with click detections on the surrounding hydrophones to estimate the Time Difference Of Arrival (TDOA) of clicks at each hydrophone with respect to the tag. This method relies on the observation that individual whales appear to produce clicks with a unique and constantly changing inter-click interval (Madsen *et al.*, 2005). For each click emitted by the tagged whale, TOE_t, a 6 s time window, from TOE_t to TOE_{t+6}, is converted into a binary 0(no click)/1(click) reference pattern with 10 ms time step resolution. This reference pattern of emitted clicks is then cross-correlated with a similarly constructed binary 0(no detection)/1(detection) 20 s window opened on each of the surrounding hydrophones from TOE_{t-10} to TOE_{t+10}. The Time of Arrival (TOA) of each emitted click on the surrounding phones is determined as the detection time resulting in the highest correlation. Thus for each click emitted, the corresponding TOA is known on the surrounding hydrophones. These TOAs are used to generate TDOAs between the surrounding hydrophones to localize the whale. Due to the narrow beamwidth of *M. densirostris*, clicks are typically detected first to one side of the direction of travel and then to the other as the animal's head scans side-to-side while echolocating. This motion results in short gaps in detections at each hydrophone. Since at least three contemporary TDOAs are needed to localize the whale's horizontal location (the animal's depth being derived from the tag) (Vincent, 2001), the TDOAs from each hydrophone were interpolated using a piecewise interpolating polynomial to fill in short data gaps. Portions of each dive in which series of clicks were detected consistently on at least three hydrophones were interpolated using this scheme. A dead-reckoned track relative to the location of the animal when tagged was calculated separately using a swim speed estimator in combination with orientation data from the tag (Zimmer *et al.*, 2005). Dead-reckoned tracks suffer from error accumulation, making them unreliable for precise positioning (Johnson *et al.*, 2009). To correct errors, the track was piecewise fit to time-aligned hydrophone localizations to produce a continuous estimate of the tagged whale's position and orientation (Ward *et al.*, 2008).

C. Whale orientation

To estimate the beam pattern, the orientation of the animal's sound source with respect to each receiving hydrophone is required. Following Zimmer *et al.* (2005), we assume that the sound source has a fixed but unknown orientation with respect to the whale's body axes. This assumption breaks down if the whale turns its head without turning the body, an action which may occur often during foraging. Nonetheless, the mean axes of the sound source over multiple clicks are likely to be stable, making the assumption reasonable in an averaged sense. The ramifications of this assumption on the derived beam pattern will be discussed in a later section. The orientation of the body axes in a geo-referenced frame can be determined as a function of time, t, from the tag accelerometer and magnetometer vectors (Johnson and Tyack, 2003; Zimmer *et al.*, 2003). To do this, the tag measurements were first rotated to account for the orientation of the tag on the animal following the methods outlined in Johnson and Tyack (2003). The tag orientation was inferred from movement data when the whale surfaced (Zimmer *et al.*, 2005). This process introduces a fixed error (i.e., a bias) of up to about $+/-5^\circ$ in the orientation. Orientation was expressed as a direction cosine matrix, W_t (Johnson and Tyack, 2003) defining the orientation of the whale's body axes with respect to the inertial (north-east-up) frame. We follow the body axis definitions in Johnson and Tyack (2003), namely, the longitudinal axis of the animal, x_w (positive in the rostral direction), the left-right axis, y_w (positive towards the right), and the ventral-dorsal axis, z_w (positive dorsally) (Johnson and Tyack, 2003).

Combining the tag location, S_t, the receiving hydrophone location, R_t, and the whale's body axes W_t, the direction vector, D_t, from the whale to the hydrophone, with respect to the whale's axes, can be calculated as

$$D_t = W_t^T(R_t - S_t). \tag{1}$$

The azimuth and elevation of the direction vector can then be derived as

$$\alpha' = \tan^{-1}\left(\frac{D_y}{D_x}\right) \tag{2}$$

and

$$\phi' = \sin^{-1}\left(\frac{D_z}{\|D\|}\right) \tag{3}$$

where $\tan^{-1}$ is the four-quadrant inverse tangent. The off-axis angle, θ, is defined as the angle between the direction vector and the whale's longitudinal axis, i.e.,

$$\theta = \cos^{-1}\left(\frac{D_x}{\|D\|}\right). \tag{4}$$

D. Hydrophone recording analysis

For each click emitted by the tagged whale and detected by a hydrophone, a corresponding 2048 sample (21 ms) sound cut was extracted from the hydrophone recording. The sound cuts were high-pass filtered at 20 kHz using a fifth-order Butterworth filter to remove low-frequency noise. The signal envelope was estimated by the magnitude of the Hilbert transformed signal (Au, 1993). The root-mean-square received level ($\mathrm{RL}_{\mathrm{rms97}}$, dB re 1 μPa) of each click was calculated using a 97% energy level criterion (Madsen and Wahlberg, 2007) within a 1 ms interval surrounding the peak point of the envelope. The time window (t_{97}, sec) was aligned to the 1.5 and 98.5 percentiles of the signal energy, i.e., the cumulative squared envelope. The centroid frequency (f_o, kHz), peak frequency (f_p, kHz), -3 dB and -10 dB bandwidths ($\mathrm{BW}_{-3\,\mathrm{dB}}$, $\mathrm{BW}_{-10\,\mathrm{dB}}$, kHz), and quality

factor ($Q_{-3\,dB}$), defined as f_o divided by $BW_{-3\,dB}$, were also calculated using the methods of Au (1993) implemented in MATLAB (Mathworks Inc., Natick, USA). These click time and spectral parameters were used to evaluate changes in click structure with off-axis angle and variation in on-axis click structure between the four tagged animals. Differences in parameters were analyzed statistically using Spearman correlation test, analysis of variance, Tukey honestly significant difference (hsd), and pairwise Wilcox tests in R (R Development Core Team, 2011).

The apparent source level (ASL), i.e., the source level back-calculated from the received level at a hydrophone at a known range, is estimated for each click using

$$\mathrm{ASL} = \mathrm{RL} + \mathrm{TL} - \mathrm{TF}(\mathrm{dB_{rms97}\ re\ 1\ \mu Pa\ @\ 1\ m}) \quad (5)$$

where TL is transmission loss (dB) and TF is the hydrophone receiving transfer function (dB), i.e., the gain of the hydrophone as a function of angle of arrival and frequency. The ASL calculation does not take into account the orientation of the whale and so provides an estimate of the source level along the direction vector (Møhl *et al.*, 2000; Madsen and Wahlberg, 2007). The beam pattern of the whale can be deduced by combining the ASL of each click with the azimuth and elevation of the corresponding direction vector.

Since the depth of the whale (d_w) is known from the pressure sensor in the tag and the depth of the hydrophone (d_h) is also known, the TL can be estimated whenever the whale can be localized. Given average clicking depths of approximately 925 m and a downward refracting sound speed profile, the TL may be influenced by the surface and seafloor boundaries especially at long ranges (Urick, 1983). A two-dimensional Gaussian eigenray bundle model (Weinberg and Keenan, 1996) with a sound velocity profile for the study area was used to determine the transition range, r_t, of 2500 m, beyond which spherical spreading is a poor approximation for the TL (Ward *et al.*, 2011). Spherical spreading, corrected for frequency dependent absorption loss, was used to estimate TL for ranges less than r_t, i.e.,

$$\mathrm{TL} = 20\log_{10}(r/r_{ref}) + \alpha * r/1000\ \mathrm{dB}. \quad (6)$$

At the average dive depth of 925 m, absorption (α) is 5.2 dB/km at a frequency of 30 kHz and water temperature of 6.9 °C (Lurton, 2002). The average absorption between 925 m animal depth and 1500 m hydrophone depth is 5.7 dB/km leading to a potential error of 1.25 dB at r_t. Beyond r_t, TL was estimated by (D'Spain *et al.*, 2006)

$$\mathrm{TL} = 20\log_{10}(r_t/r_{ref}) + 10\log_{10}(r/r_t) + \alpha * r/1000\,\mathrm{dB}. \quad (7)$$

The frequency dependent hydrophone TF (dB) was also calculated for a nominal center frequency of 30 kHz (Maripro Incorporated, 2002)

To reduce variability in the source level and beam pattern measurements due to head movements, short sequences of clicks containing potential on-axis clicks were selected for further evaluation. These sequences, termed scans, comprised clicks with increasing then decreasing ASL and likely resulted from the animal pointing towards a hydrophone briefly during foraging movement (Johnson *et al.*, 2006). For each tagged whale, all hydrophones that detected clicks were evaluated for potential scans in which at least one click was determined to be on-axis according to the following criteria: (1) ASL greater than 195 dB_{rms97}, (2) an off-axis angle, as calculated from the tag orientation sensors, of less than 25°, and (3) slant range less than 2500 m. The latter requirement ensured that the received click was subject only to spherical spreading as opposed to more complex surface or bottom interactions. A 20-click sequence centered on the on-axis click was then evaluated to determine if there was at least 30 dB between the peak and lowest ASL in the sequence. The on-axis SL is assumed to be approximately constant for the duration of the less than 7 s scan. When this last criterion was met, the scan was defined as the click sequence between the lowest ASL prior to the peak click and the lowest ASL after the peak click. Assuming that scans, as defined here, contain at least one on-axis click, the off-axis angle of the strongest click in each scan indicates the amount that the head is turned away from the body axis. To reduce error in the instantaneous beam pattern from head-turning, each scan was centered in azimuth and elevation so that the peak ASL click had a 0° off-axis angle.

E. Beam pattern

For each tagged animal, the ASLs for all detected clicks were binned in 5° azimuth × 5° elevation cells and the mean was calculated for each cell. The 5° grid was chosen to ensure that averages were performed over a suitable number of clicks in each cell, at least near the beam center. An overall average beam pattern was also obtained by combining clicks from all whales using 2.5° azimuth × 2.5° elevation bins. The objective in pooling animals is to reduce somewhat the effect of the orientation biases introduced when correcting the orientation of the tag on each whale. The beam center was taken from this composite beam pattern as the cell with the highest average ASL. The horizontal beam pattern was estimated by combining cells with elevation angles within ±2.5° of the horizontal line passing through the beam center. The vertical beam pattern was obtained in the same way using cells with azimuths within ±2.5° of a vertical line through the beam center.

A broadband circular piston model has been used as an approximation of the acoustic beam of an odontocete (Zimmer *et al.*, 2005; Au, 1993). The beam pattern predicted by this model is

$$P(x) = P_o\frac{2J_1(x)}{x} \quad \text{with} \quad x = ka\sin\theta = 2\pi\frac{a\sin(\theta)}{c}f \quad (8)$$

where P_o = source level (dB), a = piston radius (m), c = sound speed (m/s), θ = off-axis angle (rad), f = frequency (Hz), and J_1 = Bessel function of the first kind (Lurton, 2002). This model assumes that the sound source is rotationally symmetric which is unlikely from anatomical considerations but nonetheless provides a simple model for comparing beam patterns across species that may or may not have similar anatomical structures adjacent to the sound source.

The broad-band beam pattern, $B(\theta)$, is obtained by integrating $P(x)$ over frequency and applying a weighting function $W(f)$ to account for the frequency-dependent source level of clicks (Zimmer *et al.*, 2005):

$$B(\theta) = \frac{\int_{-\infty}^{\infty} P^2(\theta,f)W^2(f)df}{\int_{-\infty}^{\infty} W^2(f)df}. \quad (9)$$

$W(f)$ was created from the power spectrum of a selected on-axis, close range click. Individual scans identified using the four criteria described above were fit to the piston model to estimate the effective aperture size, a. The scan with the smallest least square error between the model and data was selected as representative for that animal.

The directivity index (DI) was obtained from the modeled beam pattern as (Au, 1993; Zimmer *et al.*, 2005),

$$\mathrm{DI} = 10\log\left[\frac{B(0)\int_0^{\pi}\sin\theta d\theta}{\int_0^{\pi} B(\theta)\sin\theta d\theta}\right] \mathrm{dB}. \quad (10)$$

The DI is a measure of the sharpness of the beam with a larger DI indicating a narrower, more directional beam.

III. RESULTS

Tags were attached to three female and one male *M. densirostris* (Table I) during 16 foraging dives. In 13 dives, the whales were sufficiently close to the hydrophone array to permit acoustic localization (Fig. 1). Some 65 000 clicks were emitted by the tagged whales during these localizable dives, of which 28 098 were detected on the bottom mounted hydrophones.

A. Foraging dive characteristics

Foraging dives had a mean vocal duration, measured from the first click during descent to the last click during ascent, of 31 min (n = 13, std = 8.3) (Table I). The dive cycle duration, defined as the time from initiating one deep foraging dive to initiating the next deep foraging dive, varied considerably from 1.4 to 5.8 h (n = 13, mean = 3.2 h, std = 1.4 h). The inter-click-interval (ICI) was estimated for each tagged whale, removing ICIs less than 0.1 s and greater than 1 s to avoid including foraging buzzes and pauses (Johnson *et al.*, 2006). Under this criterion, the mean ICI varied by individual from 0.316 to 0.354 s (Table I) with significant differences between individuals (Tukey hsd < 0.05).

The distribution of whale orientation at each click, parameterized by pitch, roll, and heading angles, and the resulting whale to hydrophone orientation relative to the whale's axes are shown in Figs. 2 and 3, respectively. Tagged whales had a fairly uniform heading distribution indicating that they were equally likely to travel in any direction. The whales' pitch distribution is slightly positively skewed indicating that whales were more likely to click with the body pitched upwards towards the surface. However, due to the location of the hydrophones on the sea-floor, clicks produced with a downward pitch were more likely to be detected.

B. Click characteristics

Scans including possible on-axis clicks were examined to assess how the waveform and spectrum changed with off-axis angle. A total of 26 scans containing 394 clicks were found. These clicks had a mean 97% energy window duration (t_{97}) of 0.38 ms (std = 0.16 ms, pooling all tagged whales) and click duration was positively correlated with off-axis angle (Spearman's rho = 0.48, $P < 0.05$). Off-axis angle was negatively correlated with ASL (Spearman's rho = −0.64, $P < 0.05$), and to a lesser degree with −3 dB bandwidth (Spearman's rho = −0.31, $P < 0.05$) and centroid frequency (Spearman's rho = −0.28, $P < 0.05$). Centroid frequency was positively correlated with both −3 dB bandwidth (Spearman's rho = 0.57, $P < 0.05$) and −10 dB bandwidth (Spearman's rho = 0.40, $P < 0.05$). The change in signal structure with off-axis angle is exemplified in the scan shown in Fig. 4, where click duration increased and centroid frequency decreased with increasing off-axis angle.

Comparison of inter-individual differences in click structure is complicated by the small number (n = 57) of assumed on-axis clicks at ranges less than 2500 m (Table II). With this set of clicks, the three animals tagged in 2007 had a similar SL of approximately 201 dB_{rms97}, while SL was lower for Md296 at 196 dB_{rms97}, but not significantly so (Tukey hsd > 0.05). Click duration, t_{97}, differed significantly between

TABLE I. Tagged beaked whale and dive vocalization characteristics. Group composition consists of ♂ female, ♀ male, and "sub" subadults of unidentified gender.

DTag	Gender	Group Size	Foraging dives (n)	Clicks produced (n)	Dive vocalization duration (min) mean (min - max)	Dive cycle duration (hr) mean (min - max)	ICI (s) mean (std)
	Adult	2			24.3	4.0	0.326
Md245	♂	1♀,1♂	3	11 679	(14.9 – 40.9)	(2.9 – 5.8)	(0.062)
	Adult	3			29.4	2.3	0.354
Md248a	♂	1♀,2♂	4	16 364	(26.8 – 31.5)	(1.4 – 2.5)	(0.075)
	Adult	3			37.6	3.5	0.336
Md248b	♀	1♀,2♂	3	18 329	(29.7 – 43.1)	(2.0 – 5.0)	(0.065)
	Adult	4			31.1	2.8	0.316
Md296	♂	2♂, 2sub	3	18 625	(26.5 – 36.0)	(1.6 – 4.0)	(0.053)

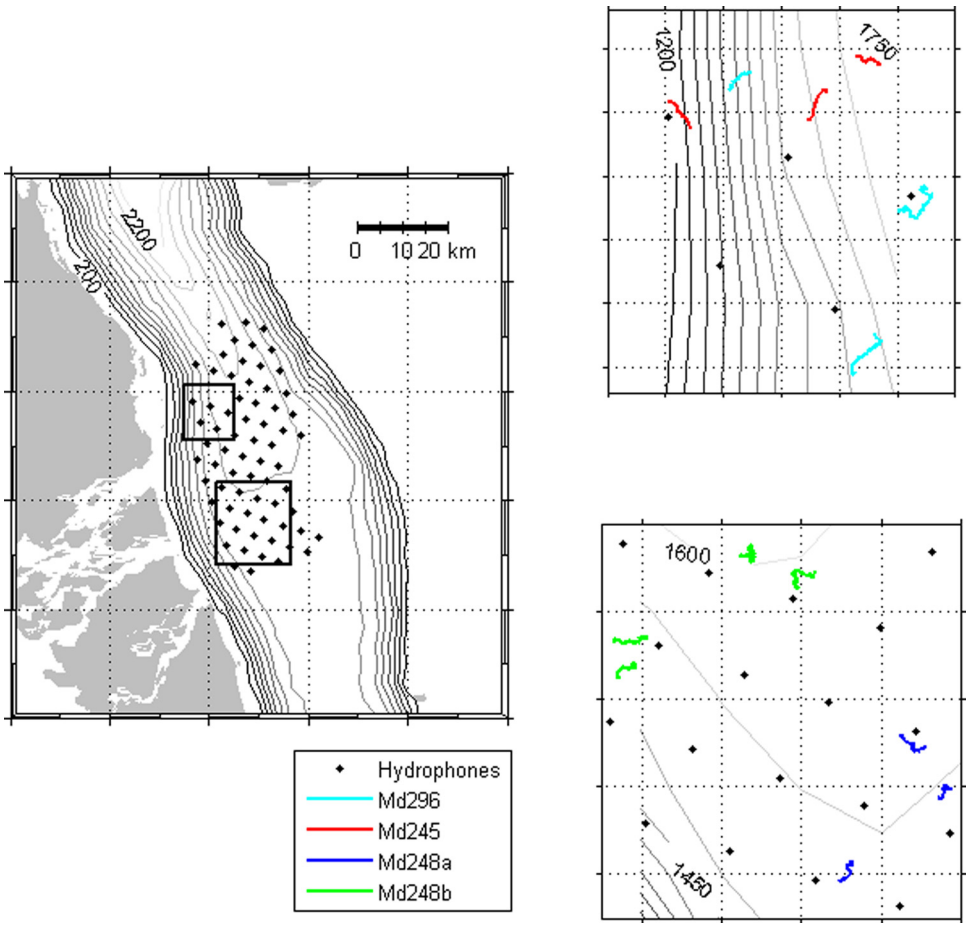

FIG. 1. (Color online) *M. densirostris* dive paths relative to the AUTEC hydrophone array. Each dive path represents a combined solution of DTag estimated track fitted to localizations of clicks from the tagged whale detected on the AUTEC hydrophones. Depth contours in meters.

Md245 and Md248b (Tukey hsd < 0.05) but not between other pairs of individuals. The -10 dB bandwidth was significantly different for all whale pairs (Tukey hsd < 0.05) except Md245 and Md248b. All on-axis clicks had a relatively flat spectrum between approximately 24 and 42 kHz, although clicks from Md296 tended to lose energy above 30 kHz, leading to a lower -3 dB bandwidth for Md296 as compared to Md245 and Md248 (Tukey hsd < 0.05).

The angle of arrival (AoA) of clicks recorded by the tag was calculated for all 16 dives (n = 72 931). The AoA indicates a range of horizontal motion of approximately 10° to either side of the mean for all whales (Fig. 5), although this likely underestimates the actual head movement as the tag is located posterior of the pivot point in the cervical vertebrae. Taking the change in AoA with time as a proxy for side-to-side scanning movement of the head, the scan rate varied between animals (Tukey hsd < 0.05) with median values of 2.4 (Md245), 3.9 (Md248a), 4.4 (Md248b), and 3.7 (Md296)°/s. The variation in AO between scans (deduced from the levels received at the tag) varied by individual animal (Fig. 6). For the same AoA, the AO varied in excess of 10 dB_{pp} for the three females and 15 dB_{pp} for the only male Md248b.

C. Beam pattern

Empirical beam patterns were generated for each animal using all 37 219 detected clicks (Fig. 7). For all whales, a concentrated region of intense source level is evident at small off-axis angles. The peak ASL occurred between 0° and -5° elevation for all animals. The peak ASL was also negatively skewed in azimuth, occurring at -5° azimuth angle for Md245, Md248a and Md248b, and at -12° azimuth angle for Md296. Clicks from all four whales were combined to produce a beam pattern plot with 2.5° by 2.5° resolution, and the vertical and horizontal beam patterns were extracted from these data (Figs. 8 and 9). The vertical beam pattern has a clear peak at negative elevation (Fig. 8), as does the horizontal beam pattern at negative azimuth (Fig. 9). These are interesting from a PAM perspective as the empirical beam patterns include the effects of head movement and variation in source level. A result of this variability is the marked difference between the average beam pattern measured at the hydrophones and a theoretical piston model fitted to a short sequence of clicks (Figs. 8 and 9).

The circular piston model that best fits the scan data from each whale is shown in Fig. 10. There is significant variation in the parameter values across individuals (Table III). Md248a gives the best model fit, yielding a 0.37 m piston diameter, approximately 10° beam width, and 26 dB DI. Averaging across all four animals, the mean estimated piston diameter is 0.28 m, with an approximately 13° beam width and 23 dB DI.

IV. DISCUSSION

Reliable information about the sound production characteristics and acoustic behavior of target species is needed to

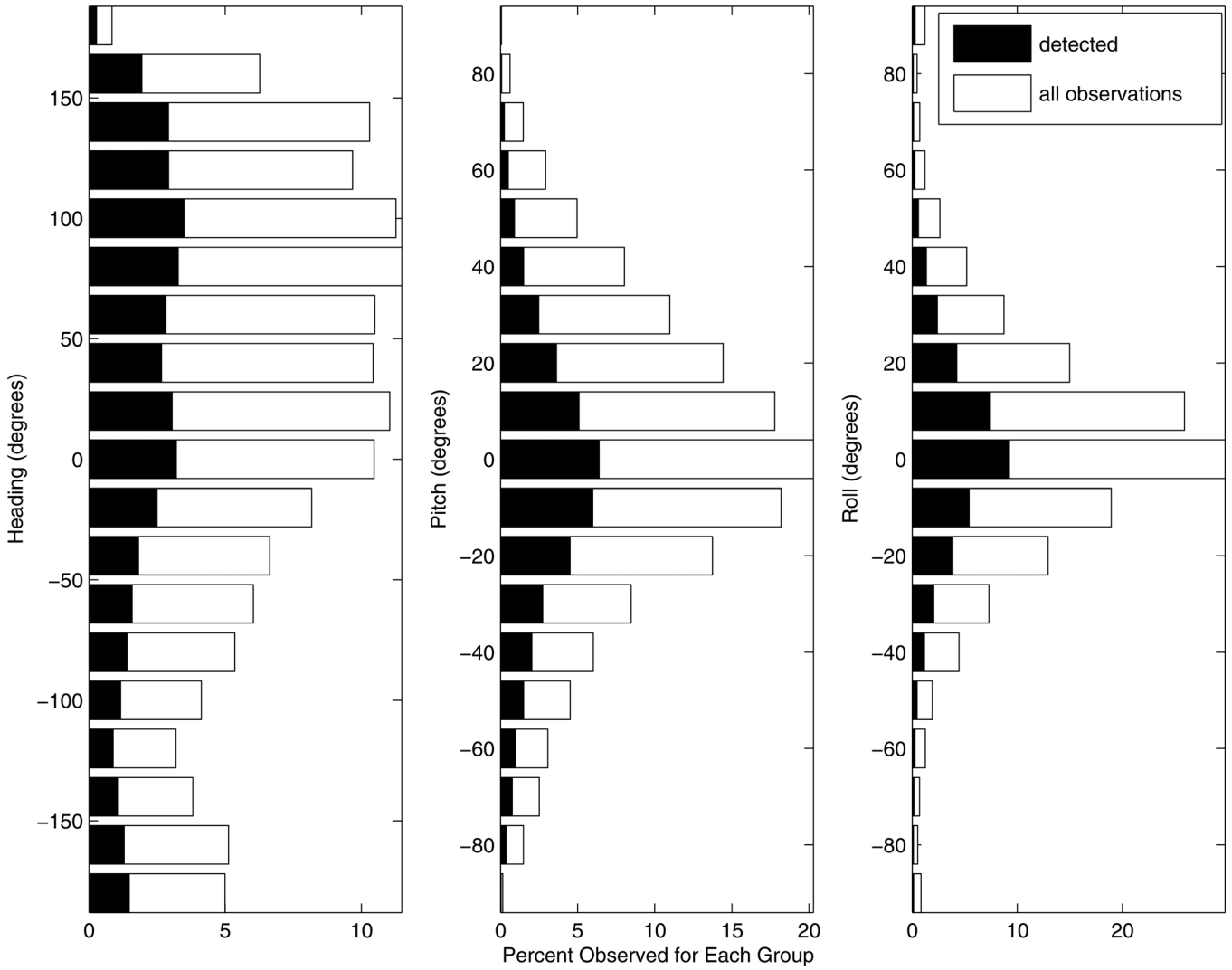

FIG. 2. *M. densirostris* heading, pitch and roll measurements corresponding to each click time for the dives analyzed. The white bars summarize observations for all clicks in this study, both detected and undetected, while the black bars show the distribution for the clicks that were detected.

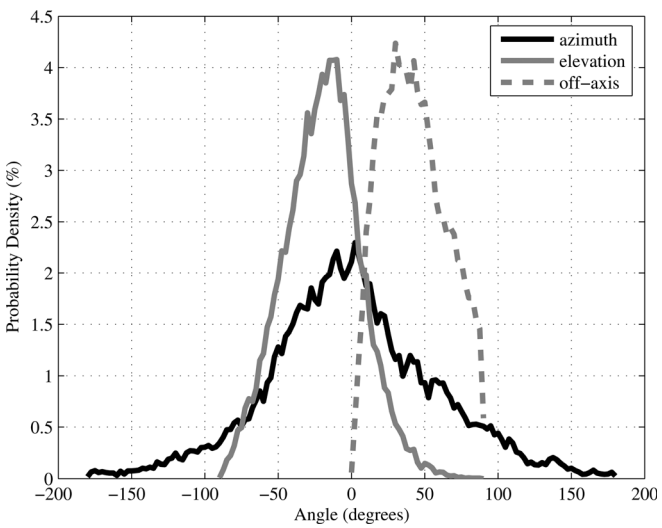

FIG. 3. Estimated probability density function of the azimuth, elevation, and off-axis angle of clicks (n = 38 629).

design and predict the performance of passive acoustic monitors. Prior reports have described the spectral and temporal characteristics of *M. densirostris* echolocation clicks (Johnson *et al.*, 2004, 2006; Ward *et al.*, 2008; Aguilar de Soto *et al.*, 2011) but only vague information about the source level and beam pattern has been available. These latter data are critical to predict the probability of detection of a PAM system and to establish the density of receivers required to achieve a given level of performance. Moreover, much of the published data on *M. densirostris* has come from a small resident population in the Canary Islands and there is a need to verify that these data apply to populations in other areas. Here we report sound and movement recordings from four *M. densirostris* in the Bahamas that both confirm the click characteristics of this species and provide the first estimates of source level and beam pattern. The number of individuals in the study is admittedly small, but the difficulties involved in tagging beaked whales and the urgent need to establish effective mitigation measures for this vulnerable species make the data valuable.

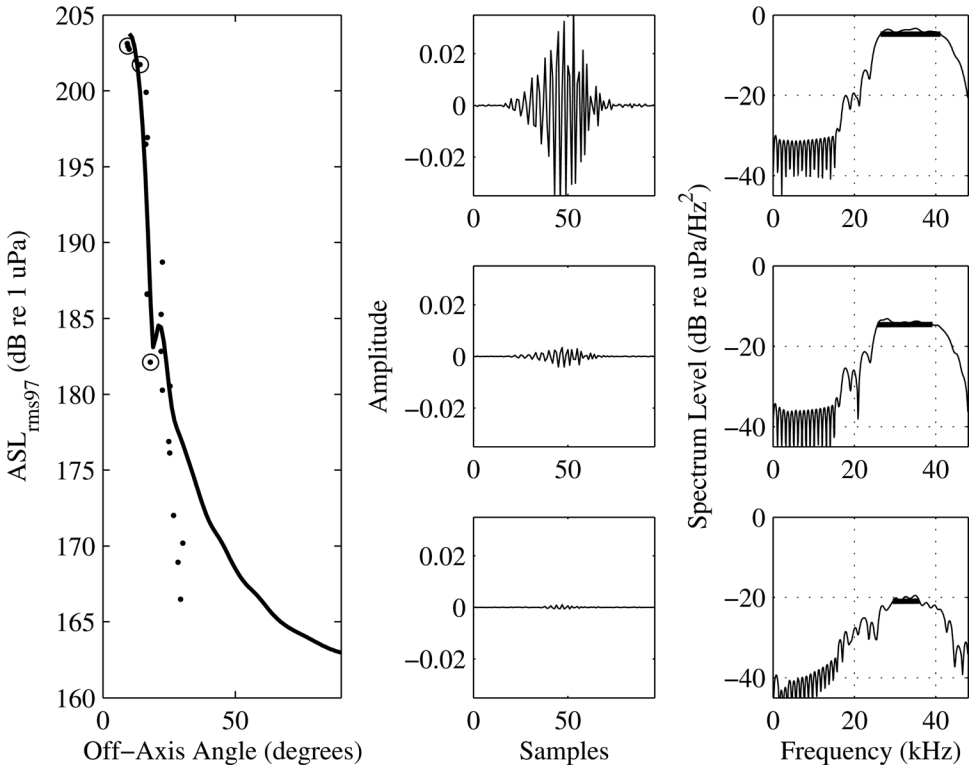

FIG. 4. Example of a click sequence recorded on a hydrophone where the body-axis is likely not aligned with the acoustic axis of the tagged animal. The plot to the left indicates measured versus modeled beam pattern during a single scan across a hydrophone. Note that the maximum source level is recorded approximately 10° off-center. The points indicate the ASL recorded for each click during the scan. The solid black line is the fitted piston model transmission beam pattern. The amplitude and frequency spectrum of the three circled point measurements illustrating clicks from on-axis to progressively off-axis are shown in the plots to the right. Solid lines on the spectra indicate the 3 dB bandwidth.

On-axis source levels for the four animals, back-calculated from signals received at hydrophones within 2500 m of each animal, varied between 196 dB and 201 dB re 1μPa RMS with a median value of 201 dB. These source levels were obtained with a 48 kHz bandwidth recording system which may be too limited in frequency to capture the entire click spectrum. However, the upper −10 dB frequencies of the clicks recorded here are enough below the cut-off frequency of the system as to suggest that most of the energy was sampled. Clicks from the same species recorded in the Canary Islands had a slightly higher median −10 dB frequency of 50 kHz, which may be specific to the population there, or may be a result of shorter propagation distances in that study and therefore less high-frequency attenuation. In either case, clicks had little energy above 48 kHz and so a wider bandwidth recording is unlikely to yield a very different source level. For clicks recorded with wide bandwidth and good SNR, the RMS-97 level is about 11 dB less than the peak-to-peak level so the results reported here are compatible with the broad 200–220 dB re 1μPa peak-to-peak range estimated in Johnson *et al.* (2004).

Other spectral and temporal characteristics of clicks recorded here are also broadly similar to those reported from the Canary Islands. Clicks comprised an upwards FM sweep with a slightly longer 97% energy duration (0.32 ms here vs 0.27 ms in the Canary Islands) and a lower centroid frequency (33 kHz here vs 38 kHz in the Canary Islands). As with the source level, these minor differences may result from greater absorption at high frequencies due to longer path lengths than in the Johnson *et al.* (2006) study. Thus,

TABLE II. Click characteristics for peak ASL clicks recorded on the bottom mounted hydrophones within 2500 m slant range of each whale: SL_{rms97} (root-mean-square source level using a 97% energy level criterion), SL_{pp} (peak to peak source level), t_{rms97} (time window length for 97% energy), f_o (centroid frequency), f_p (peak frequency), $BW_{-3\,dB}$ and $BW_{-10\,dB}$ (−3 dB and −10 dB bandwidths), and $Q_{-3\,dB}$ (quality factor defined as f_o divided by $BW_{-3\,dB}$).

DTag	Md296	Md245	Md248a	Md248b
n (clicks)	5	22	3	27
range (m)	1875 (1654–2047)	1741 (1083–2132)	1734 (1040–2319)	1923 (1136–2483)
SL_{rms97} (dB)	196.2 (195.1–198.8)	201.0 (195.4–208.0)	201.1 (200.1–202.6)	200.7 (195.2–203.5)
SL_{pp} (dB)	207.6 (206.3–210.1)	212.2 (207.0–219.3)	212.7 (211.8–214.0)	211.6 (207.1–214.3)
t_{rms97} (ms)	0.32 (0.30–0.33)	0.32 (0.25–0.38)	0.32 (0.32–0.32)	0.28 (0.27–0.30)
f_{pk} (kHz)	29.8 (27.0–34.4)	32.7 (26.2–35.4)	31.5 (27.0–9.8)	32.2 (26.5–34.6)
f_o (kHz)	32.1 (30.8–33.4)	33.9 (31.5–35.8)	33.5 (32.3–35.4)	32.8 (31.1–34.3)
BW −3 dB (kHz)	11.0 (7.8–14.3)	12.4 (8.6–15.4)	13.8 (10.4–16.7)	12.5 (8.7–14.1)
BW −10 dB (kHz)	17.6 (16.3–18.7)	18.4 (17.0–19.2)	19.4 (18.9–20.3)	18.1 (16.8–18.9)
Lower −10 dB (kHz)	24.5 (24.4–24.7)	25.1 (23.5–26.3)	24.4 (24.4–24.5)	24.5 (23.8–24.9)
Upper −10 dB (kHz)	42.1 (40.7–43.3)	43.5 (41.8–44.2)	43.8 (43.4–44.7)	42.6 (40.8–43.3)
Q	2.9	2.7	2.4	2.6

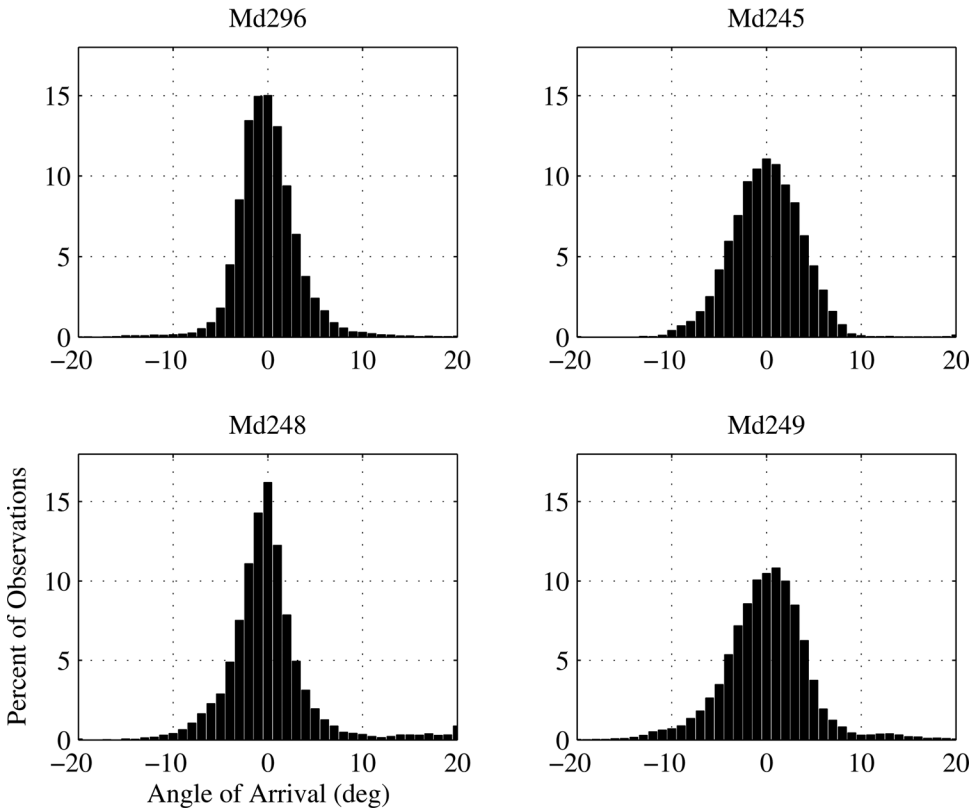

FIG. 5. Angle of arrival (AOA) variation of clicks recorded on stereo DTAGs on each animal. The mean AOA is removed from each plot.

although the data sets from the two locations are small, there is no strong indication of population-level differences in vocal characteristics.

The bulk of the energy in *M. densirostris* clicks coincides with a frequency range of low ambient noise making these clicks especially suitable for PAM. Detection ranges up to 6500 m have been obtained in quiet ocean conditions such as occur in the TOTO (Ward *et al.*, 2008). This detection range is longer than the spacing between hydrophones in the AUTEC bottom-mounted array leading to a high

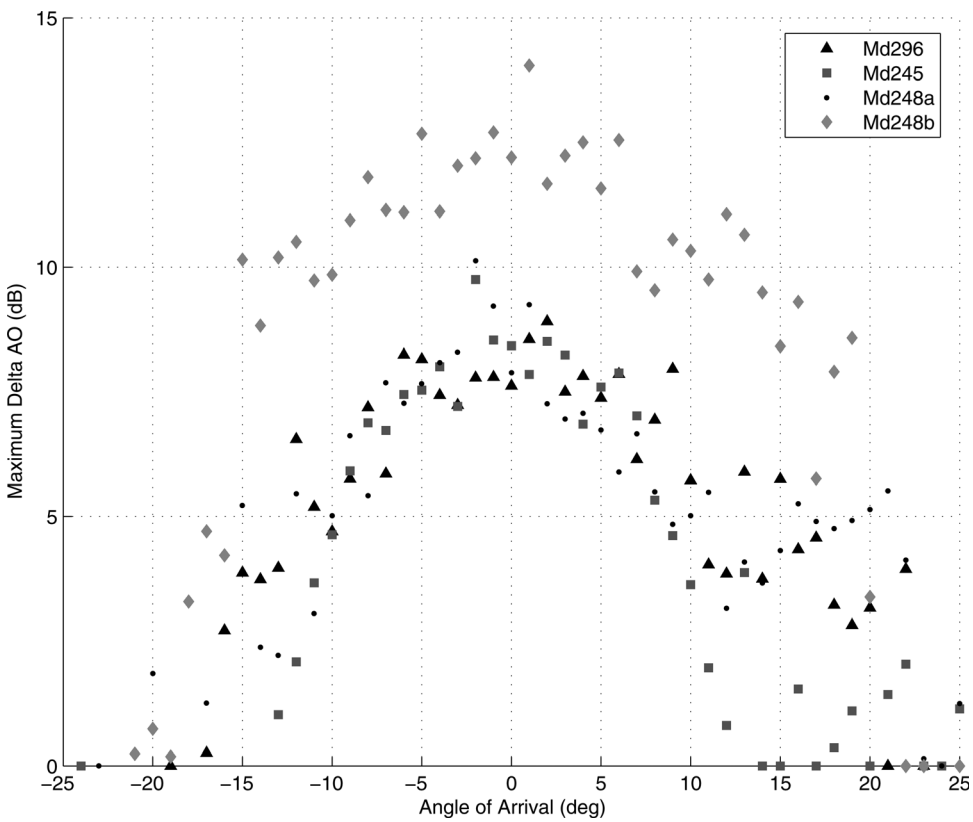

FIG. 6. Estimated probability density function of AOA for each tagged whale. The mean AOA is removed from each plot.

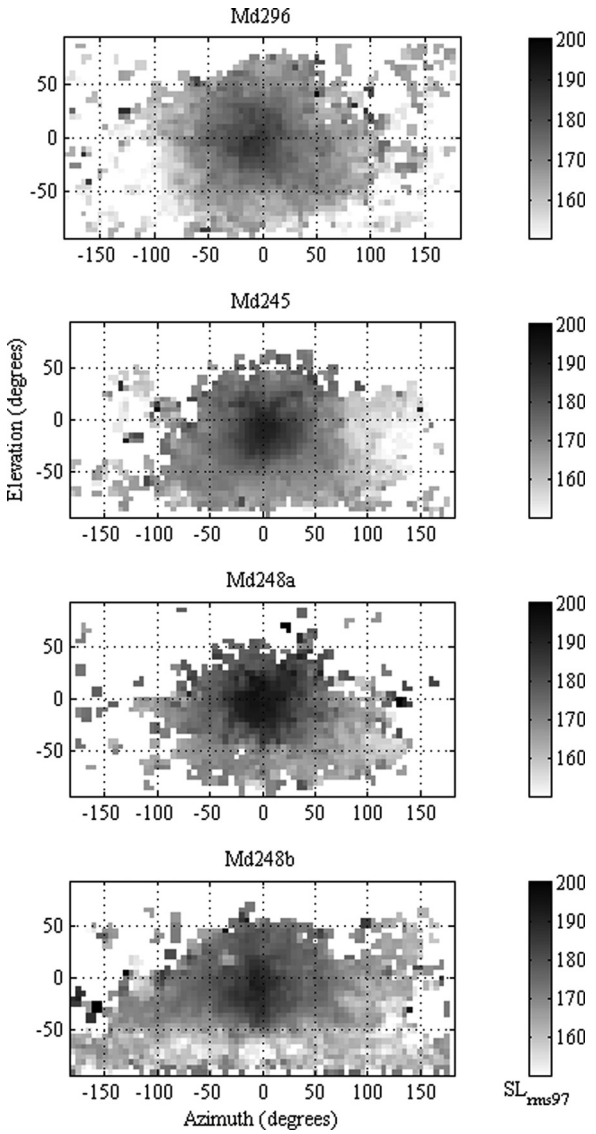

FIG. 7. Estimated transmission beam pattern for each tagged whale. The mean ASLrms97 level in each 5° by 5° cell is displayed. ASL units are dB re 1 μPa at 1 m. White cells indicate that no clicks were received at the corresponding azimuth and elevation.

probability of detecting on-axis clicks from foraging beaked whales in TOTO, at least when there are no interfering noise sources. For PAM a more useful measure of detection performance is the potential number of clicks that would be detected from arbitrarily oriented animals during the course of a foraging dive. This requires information on the movement of animals while foraging and on their transmission beam pattern. This information is also required to predict the performance of sparser monitoring arrays or of acoustic localization systems.

The new data presented here provide a basis for more accurate simulations of detector performance as a function of array size and placement building on the work of Zimmer *et al*. (2008). The mean DI of 23 dB, reported here, indicates a narrow, directional beam, but the volume of water ensonified over a complete foraging dive is nonetheless large given the combined effects of foraging movements, independent head movements, and high source levels. Along the meandering 15 to 40 min foraging dives, tagged animals traveled with equal probability in all directions, clicking consistently with an approximately 0.33 s ICI. While searching for prey, the head scans horizontally over an angular range of $\pm 10°$ at a mean rate of 3.6°/s further increasing the ensonified volume. Vertical head scans may also occur but were unobservable with the two-hydrophone array on the tags used here.

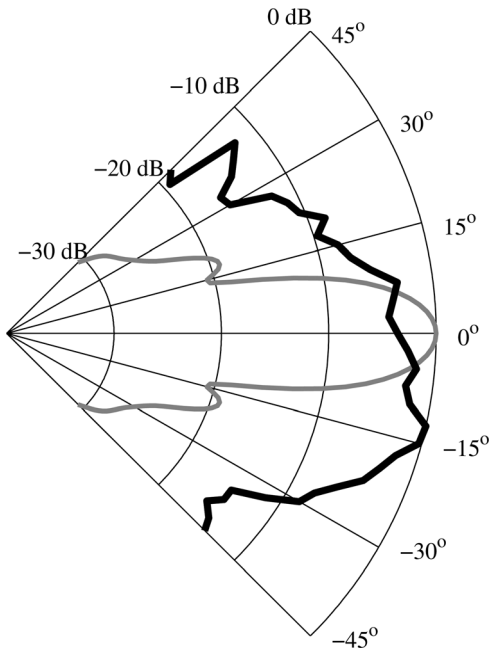

FIG. 8. Cumulative vertical beam pattern using all clicks received between 0° and 2.5° azimuth. Piston model results for Md248b overlaid.

The capability to count and localize individuals within a foraging group is important for abundance studies (Marques *et al*., 2009) and studies of the behavioral impact of sound (McCarthy *et al*., 2011; Tyack *et al*., 2011). The most

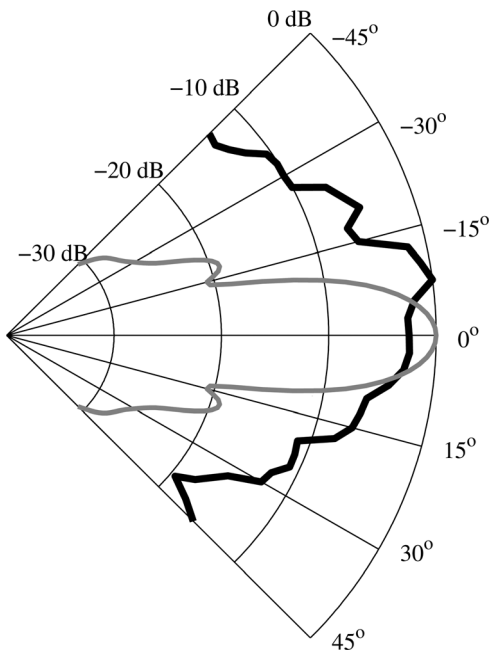

FIG. 9. Cumulative horizontal beam pattern using all clicks received between 0° and 2.5° elevation. Piston model results for Md248b overlaid.

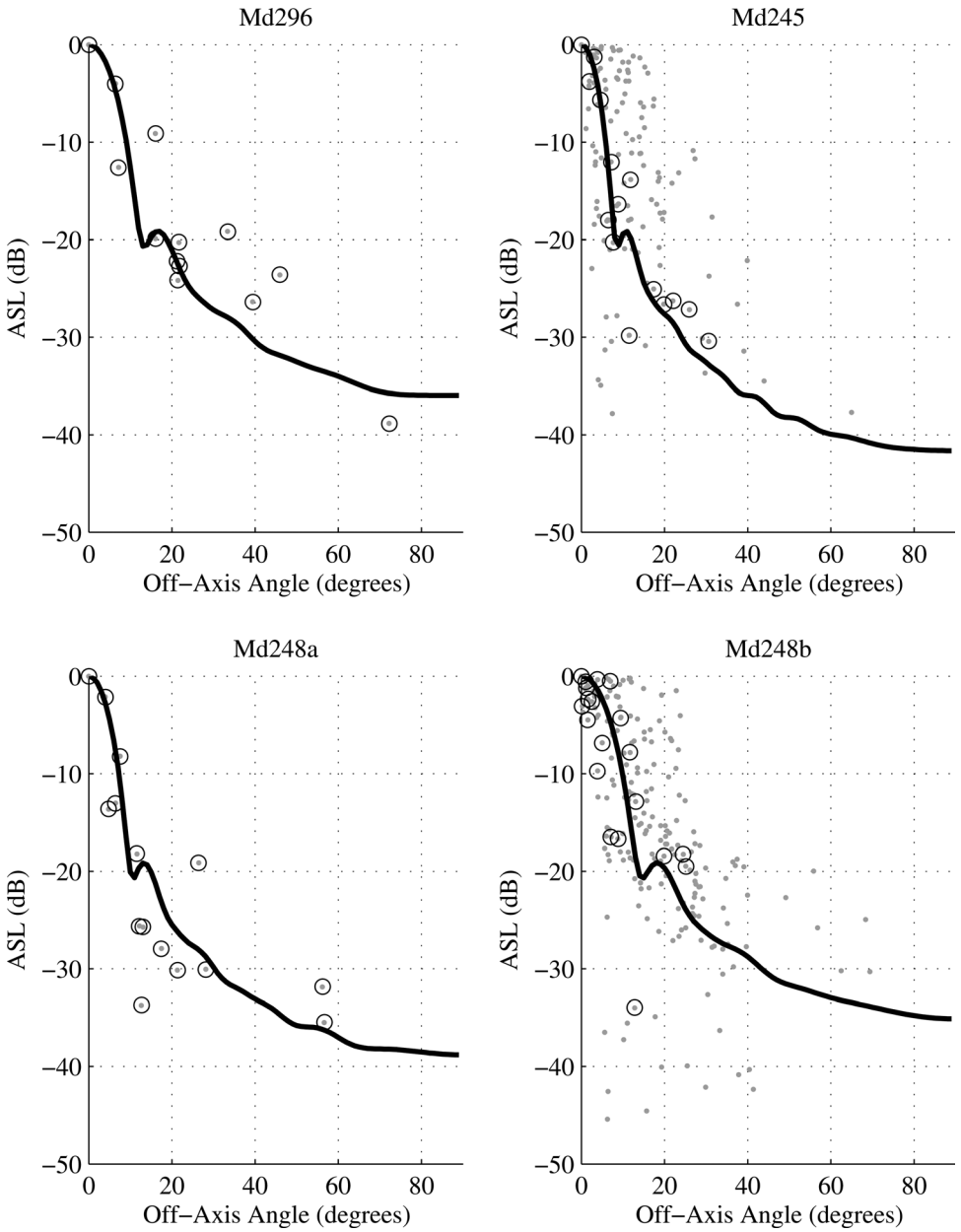

FIG. 10. Circular piston model results for the four tagged whales. Gray dots indicate ASLs centered to 0° off-axis angle from scans selected using the four criteria (see methods). Black circles indicate the ASLs measured in the single scan for each whale with the best piston model fit.

straightforward way to localize an individual is to detect a click on multiple hydrophones (≥3 for horizontal localization or ≥4 hydrophones for 3D localization) and use the time delays of arrival (TDOA) to estimate the source position (Vincent, 2001). While the cumulative ensonified volume in a dive is large, the volume ensonified by each click is relatively small given the mean beam width of 13° (Table III). A consequence of this directionality is that single clicks were rarely detected on more than one hydrophone. As a result, more complex localization methods that interpolate TDOA over sequences of clicks received on multiple hydrophones are needed. Even for nominally on-axis clicks, the probability of detection may be less than expected. The probability of detection, P_d, of a single click over all off-axis angles was estimated, using the same dataset, by Marques *et al.* (2009) to be 0.032 for clicks produced within 8 km of a hydrophone. The P_d decreased significantly with increasing off-axis angle, an expected result of the narrow beam pattern observed here. An unexpected result in the Marques *et al.* (2009) study was that the maximum value of P_d for close on-axis clicks was 0.8 rather than 1. In the Marques *et al.* (2009) study, the off-axis angle was determined exclusively from the orientation data of the DTag. Our results show a +/−10° range of head movement independent of the body orientation as well as

TABLE III. *M. densirostris* circular piston model beam pattern characteristics based on the best fit scan for each tagged whale.

DTag	Clicks (n)	Piston Diameter (m)	Beamwidth (deg)	DI (dB)	Error (dB)
Md245	13	0.24	15.0	21.8	1.39
Md248a	15	0.37	9.7	25.6	1.04
Md248b	15	0.30	12.0	23.8	1.58
Md296	20	0.22	16.4	21.0	1.38
mean		0.28	13.3	23.0	

slowly varying SL from scan to scan in excess of 10 dB_{pp} both of which lower the probability of detecting clicks from an animal even though its body may be aligned towards the hydrophone.

The estimated beam patterns of the four *M. densirostris* suggest a beam center that is slightly downward and to the left of the 0-azimuth, 0-elevation point (Fig. 7). The off-center axis may be the result of several factors. As in many odontocetes, *M. densirostris* have notably asymmetrical cranial structures involving both bone and soft tissues that influence sound radiation (Au *et al.*, 1995; Cranford *et al.*, 2008). Similar off-center beams in *Tursiops*, *Delphinapterus* and *Pseudorca* have been associated with asymmetric anatomical structures around the melon visualized in MRI and CT scans (Au *et al.*, 1995). The mean beam pattern also integrates the effect of head movement independent of the body axis and so any lateralization of head turns, e.g., a tendency to turn right more than left, would translate into a net displacement of the mean beam center. A third and simpler possibility is that the apparent beam center is affected by errors in the way the orientation of the animal is deduced from the tag sensor data. A key step in orientation estimation is to predict how the tag is oriented on the animal (Johnson and Tyack, 2003). The method used to achieve this makes assumptions about the movements of animals when respiring at the surface (Zimmer *et al.*, 2005), e.g., that they adopt zero pitch and roll angles at the moment of inhalation. If the animal's body is consistently curved in the same way at this moment, then the tag orientation may not match the overall body orientation potentially introducing biases in pitch, roll and heading which could be of the order of 10°, comparable to the off-center angles reported here. Anatomical structures may, however, influence another finding of the current study. *M. densirostris* rostral bone has one of the highest densities, mineral content, and compactness measured in mammal bone (DeBuffrenil *et al.*, 2000). Males have a larger rostral complement and denser mesorostral bone (Besharse, 1971) resulting in a deeper, wider and shorter rostrum than in the female. Although the on-axis source level was similar across the four animals for on-axis clicks, the only male in the study, Md248b, had much higher off-axis ASL than the three females.

Fitting a circular piston model to scans from the four animals gave a mean piston diameter of 0.28 m, approximately 70% of the 0.40 m diameter estimated for a single *Z. cavirostris* by Zimmer *et al.* (2005). While the size of the tagged animals was not estimated, comparing the maximum skull width of the two species indicates that *M. densirostris* (data from Besharse, 1971) are on average 60% the size of *Z. cavirostris* (data from Hardy, 2005), roughly matching the difference in piston diameter. Head diameter measurements for *M. densirostris* taken at mid-orbit, which is approximately coincident with the widest width of the melon, were 0.31, 0.31, and 0.40 m for a juvenile male and 2 adult males, respectively (D. Ketten, personal communication). For delphinids, the relationship of DI and 3-dB beamwidth has been shown to be a function of the head diameter divided by the wavelength corresponding to the peak frequency [Au *et al.*, 1999, Eq. (2) and (3)]. Using these equations and the average head diameter for the two adults, 0.36 m, as a proxy for piston diameter, and a peak frequency of 34 kHz, the predicted DI is 23.1 dB with a corresponding 3-dB beamwidth of 19.0°. The predicted DI is in close agreement with the values measured here although the predicted beamwidth is somewhat greater than measured here. The directivity of a transducer beam is generally proportional to the size of the radiating surface relative to the wavelength (Au, 1993). Compared to other odontocete species for which DI has been measured, *M. densirostris* produces clicks with lower center frequency. This results in a lower DI than would be otherwise expected when comparing against the smaller *T. truncatus* (DI = 25.8) and the larger *D. leucas* (DI = 39.8) (Table IV; Au *et al.*, 1999; Zimmer *et al.*, 2005). The larger *Z. cavirostris* also produces clicks with a slightly higher center frequency resulting in an estimated DI of 30 dB (Zimmer *et al.*, 2005) and a beamwidth which, at 6°, is substantially smaller than the 13° beam estimated here for *M. densirostris*. Such a narrow beam may have an ecological significance relating to prey choice and/or habitat conditions, but this has yet to be determined.

A secondary objective of this study was to determine if any of the measured acoustic characteristics could be used to distinguish individuals and so aid in determining the number of animals in a group. While the mean ICIs differed significantly between the tagged animals, the effect size was small. Foraging movements lead to frequent gaps in detections at any one hydrophone, making ICI estimation from hydrophone detections alone unreliable. Given the narrow beam

TABLE IV. Acoustic transmission characteristics of *P. phocoena* (Au *et al.*, 1999), *H. ampullatus* (Wahlberg *et al.*, 2011), *M. densirostris* (this paper), *Z. cavirostris* (Zimmer, 2005), *Pseudorca crassidens* (Au *et al.*, 1995; Au, 1993), *Tursiops truncatus* (Au, 1993) and *Delphinapterus leucas* (Au, 1993; Au *et al.*, 1987). *H. ampullatus*, *M. densirostris*, and *Z. cavirostris* DI and beam width estimated by fitting piston model to measured ASL. d/λ is the head diameter of the animal divided by the wavelength corresponding to the peak frequency.

	Head Diameter (cm)	SL_{pp} (dB re μPa)	F_{pk} (kHz)	DI (dB)	d/λ	3-dB beam width (degrees)	$Q_{-3\,dB}$
Phocoena phocoena	14.8	172	127	22.1	12	16.4	7.8
Tursiops truncatus	28.6	228	117	25.8	22	9.9	2–3
Delphinapterus leucas	39.8	218	110	32.6	29	6.5	2.8
Pseudorca crassidens	38.2	213	104	28.5	26	8.0	5.3
Hyperoodon ampullatus	92.0	203	55	18.3	25	19.8	2.5
Mesoplodon densirostris	35.7	217	34	23.1	8	19.0	2.4–2.9
Ziphius cavirostris	60	214	45	30.0	18	12.6	4

width and similar on-axis source level across individuals reported here, a simple way to estimate the number of individuals clicking may be to find concurrent scans on different hydrophones. Additionally, the click with the peak RL within each scan could be used to provide a rough estimate of the range to an animal and, when combined with coincident detections on another hydrophone, the bearing. Given the typically small group size of foraging *M. densirostris*, this may be sufficient information to count individuals. Although more complex, a combined acoustic and behavioral model incorporating the ASL, beam width, scan rate, and time-of-arrival (TOA) on the hydrophones would likely provide more reliable group size estimates. Given the similarity of on-axis click time-frequency characteristics, differentiating individuals based on signal structure alone from the wide baseline hydrophones appears to be unlikely.

ACKNOWLEDGMENTS

These data were collected during the 2006 Bahamas Species Verification Test and 2007 Behavioral Response Study funded by the Environmental Readiness Division of the U.S. Navy (N45), U.S. Office of Naval Research, U.S. Chief of Naval Operations Submarine Warfare Division (Undersea Surveillance IWS5) and Strategic Environmental Research and Development Program. We would like to thank the entire field team that participated in the 2007 BRS for supporting the effort that provided the data for this study. This work was funded by two partners under the National Oceanographic Partnership Program: the Ocean Acoustics Program of the U.S. National Marine Fisheries Service, Office of Protected Resources, and the International Association of Oil and Gas Producers Joint Industry Programme on Exploration and Production Sound and Marine Life. Research permits were issued to John Boreman (US NMFS 1121-1900), Peter Tyack (US NMFS 981-1578), and Ian Boyd (Bahamas permit #02/07). The tagging research was approved by the WHOI and Bahamas Marine Mammal Research Organisation Institutional Animal Care and Use Committees. M.J. and P.T. are supported by the Marine Alliance for Science and Technology Scotland.

Aguilar de Soto, N., Madsen, P. T., Tyack, P., Arranz, P., Marrero, J., Fais, A., Revelli, E., and Johnson, M. (**2011**). "No shallow talk: Cryptic strategy in the vocal communication of Blainville's beaked whales," Mar. Mammal Sci. doi:10.1111/j.1748-7692.2011.00495.x

Au, W., Penner, R. H., and Tenner, C. W. (**1987**). "Propagation of Beluga echolocation signals," J. Acoust. Soc. Am. **92**, 807–813.

Au, W., Pawloski, J. L., Nachtigall, P. E., Blonz, M., and Gisiner, R. C. (**1995**). "Echolocation signals and transmission beam pattern of a false killer whale (*Pseudorca crassidens*)," J. Acoust. Soc. Am. **98**, 51–59.

Au, W. W. L. (**1993**). *The Sonar of Dolphins* (Springer, New York), 277 p.

Au, W. W. L., Kastelein, R., Rippe, T., and Schooneman, N. M. (**1999**). "Transmission beam pattern and echolocation signals of harbor porpoise (*Phocoena phocoena*)," J. Acoust. Soc. Am. **106**, 3699–3705.

Barlow, J. (**1999**). "Trackline detection probability for long diving whales," in *Marine Mammal Survey and Assessment Methods*, edited by G. W. Garner, S. C. Amstrup, J. L. Laake, B. J. F. Manley, L. L. McDonald, and D. G. Robertson (Balkema, Netherlands), pp. 209–221.

Baumann-Pickering, S., Wiggins, S. M., Roth, E. H., Roch, M. A., Schnitzler, H., and Hildebrand, J. A. (**2010**). "Echolocation signals of a beaked whale at Palmyra Atoll," J. Acoust. Soc. Am. **127**, 3790–3799.

Besharse, J. C. (**1971**). "Maturity and sexual dimorphism in the skull, mandible, and teeth of the beaked whale, *Mesoplodon densirostris*," J. Mammal. **52**, 297–315.

Boyd, I. L., Claridge, D. E., Clark, C. W., Southall, B. L., and Tyack, P. L. (**2007**). "Behavioral Response Study Cruise Report (BRS-2007)," http://www.nmfs.noaa.gov/pr/pdfs/acoustics/brs2007_finalcruisereport.pdf (Last viewed June 1, 2012).

Cranford, T. W., Krysl, P., and Hildebrand, J. A. (**2008**). "Acoustic pathways revealed: Simulated sound transmission and reception in Cuvier's beaked whale (*Ziphius cavirostris*)," Bioinsp. Biomim. **3**, 1–10.

D'Amico, A. D., Gisiner, R., Ketten, D. R., Hammock, J. A., Johnson, C., Tyack, P., and Mead, J. (**2009**). "Beaked whale strandings and naval exercises," Aquat. Mammals **35**, 452–472.

DeBuffrenil, V., Zylberberg, L., Traub, W., and Casinos, A. (**2000**). "Structural and mechanical characteristics of the hyperdense bone of the rostrum of *Mesoplodon densirostris* (Cetacea, Ziphiidae): Summary of recent observations," Historical Bio. **14**, 57–65.

DiMarzio, N. A., Moretti, D., Ward, J., Morrissey, R., Jarvis, S., Izzi, A., Johnson, M., Tyack, P., and Hansen, A. (**2008**). "Passive acoustic measurement of dive vocal behavior and group size of Blainville's beaked whale (*Mesoplodon densirostris*) in the Tongue of the Ocean (TOTO)," Can. Acoust. **36**, 166–173.

D'Spain, G. L., D'Amico, A., and Fromm, D. M. (**2006**). "Properties of the underwater sound fields during some well documented beaked whale mass stranding events," J. Cetacean Res. Manage. **7**, 223–238.

Gillespie, D., Dunn, C., Gordon, J., Claridge, D., Embling, C., and Boyd, I. (**2009**). "Field recordings of Gervais' beaked whales *Mesoplodon europaeus* from the Bahamas," J. Acoust. Soc. Am. **125**, 3428–3433.

Hardy, M. (**2005**). "Extent, development and function of sexual dimorphisms in the skulls of the bottlenose whales (*Hyperoodon spp.*) and Cuvier's beaked whale (*Ziphius cavirostris*)," M.S. thesis, School of Biological Sciences, University of Wales, Bangor.

Johnson, M., Aguilar de Soto, N., and Madsen, P. T. (**2009**). "Studying the behaviour and sensory ecology of marine mammals using acoustic recording tags: a review," Mar. Ecol. Prog. Ser. **395**, 55–73.

Johnson, M., Madsen, P. T., Zimmer, W. M. X., Aguilar de Soto, N., and Tyack, P. L. (**2004**). "Beaked whales echolocate on prey," Proc. R. Soc. London B **271**(Suppl. 6), S383–S386.

Johnson, M., Madsen, P. T., Zimmer, W. M. X., Aguilar de Soto, N., and Tyack, P. L. (**2006**). "Foraging Blainville's beaked whales (*Mesoplodon densirostris*) produce distinct click types matched to different phases of echolocation," J. Exp. Biol. **209**, 5038–5050.

Johnson, M. P., and Tyack, P. (**2003**). "A digital acoustic recording tag for measuring response of wild marine mammals to sound," IEEE J. Oceanic Eng. **28**, 3–12.

Lurton, X. (**2002**). *An Introduction to Underwater Acoustics: Principles and Applications* (Praxis Publishing, U.K.), pp. 165–168.

Madsen, P. T., Johnson, M., Aguilar de Soto, N., Zimmer, W. M. X., and Tyack, P. (**2005**). "Biosonar performance of foraging beaked whales (*Mesoplodon densirostris*)," J. Exp. Biol. **208**, 181–194.

Madsen, P. T., and Wahlberg, M. (**2007**). "Recording and quantification of ultrasonic echolocation clicks from free-ranging toothed whales," Deep Sea Res. **54**, 1421–1444.

Maripro Incorporated (**2002**). Atlantic Undersea Test and Evaluation Center (AUTEC) Hydrophone Replacement Program (AHRP) training materials/training program, Contract No. N66604-97-C-0347 (Maripro Incorporated, Goleta, CA), 141 p.

Marques, T. A., Thomas, L., Ward, J., DiMarzio, N., and Tyack, P. (**2009**). "Estimating cetacean population density using fixed passive acoustic sensors: An example with beaked whales," J. Acoust. Soc. Am. **125**, 1982–1994.

McCarthy, E., Moretti, D., Thomas, L., DiMarzio, N., Morrissey, R., Jarvis, S., Ward, J., Izzi, A., and Dilley, A. (**2011**). "Changes in spatial and temporal distribution and vocal behavior of Blainville's beaked whales (*Mesoplodon densirostris*) during multiship exercises with mid-frequency sonar," Mar. Mammal Sci. **27**, E206–E226.

Mellinger, D. K., Stafford, K. M., Moore, S. E., Dziak, R. P., and Matsumoto, H. (**2007**). "An overview of fixed passive acoustic observation methods for cetaceans," Oceanography **20**, 36–45.

Møhl, B., Wahlberg, M., Madsen, P. T., Miller, L. A., and Surlykke, A. (**2000**). "Sperm whale clicks: Directionality and source level revisited," J. Acoust. Soc. Am. **107**, 638–648.

Nosal, E. M., and Frazer, L. N. (**2007**). "Sperm whale three-dimensional track, swim orientation, beam pattern, and click levels observed on bottom-mounted hydrophones," J. Acoust. Soc. Am. **122**, 1969–1978.

Rasmussen, M. H., Wahlberg, M., and Miller, L. A. (**2004**). "Estimated transmission beam pattern of clicks recorded from free-ranging white-beaked dolphins (*Lagenorhynchus albirostris*)," J. Acoust. Soc. Am. **116**, 1826–1831.

R Development Core Team (**2011**). "R: A Language and Environment for Statistical Computing," R Foundation for Statistical Computing, Vienna, Austria, http://www.R-project.org (Last viewed June 1, 2012).

Tyack, P. L., Johnson, M. P., Zimmer, W. M. X., Aguilar de Soto, N., and Madsen, P. T. (**2006**). "Acoustic behavior of beaked whales, with implications for acoustic monitoring," IEEE Oceans Conf. Proc. **2006**, 1–6.

Tyack, P. L., Zimmer, W. M. X., Moretti, D., Southall, B. L., Claridge, D. E., Durban, J. W., Clark, C. W., D'Amico, A., DiMarzio, N., Jarvis, S., McCarthy, E., Morrissey, R., Ward, J., and Boyd, I. L. (**2011**). "Beaked whales respond to simulated and actual Navy sonar," PLoS One **6**, e17009.

Urick, R. J. (**1983**). *Principles of Underwater Sound* (McGraw-Hill, New York), 423 p.

Vincent, H. (**2001**). "Models, algorithms, and measurements for underwater acoustic positioning," Ph.D. dissertation, Univ. of Rhode Island, Kingston, RI.

Wahlberg, M., Jensen, F. H., Aguilar de Soto, N., Beedholm, K., Bejder, L., Oliveira, C., Rasmussen, M., Simon, M., Villadsgaard, A., and Madsen, P. T. (**2011**). "Source parameters of echolocation clicks from wild bottlenose dolphins (*Tursiops aduncus* and *Tursiops truncatus*)," J. Acoust. Soc. Am. **130**, 2263–2274.

Ward, J., Jarvis, S., Moretti, D., Morrrissey, R., DiMarzio, N., Johnson, M., Tyack, P., Thomas, L., and Marques, T. (**2011**). "Beaked whale (*Mesoplodon densirostris*) passive acoustic detection in increasing ambient noise," J. Acoust. Soc. Am. **129**, 662,

Ward, J., Morrissey, R., Moretti, D., DiMarzio, N., Jarvis, S., Johnson, M., Tyack, P., and White, C. (**2008**). "Passive acoustic detection and localization of *Mesoplodon densirostris* (Blainville's beaked whale) vocalizations using distributed bottom-mounted hydrophones in conjunction with a digital tag recording," Can. Acoust. **36**, 60–66.

Watwood, S., Miller, P. O., Johnson, M., Madsen, P. T., and Tyack, P. L. (**2006**). "Deep-diving foraging behavior of sperm whales (*Physeter macrocephalus*)," J. Anim. Ecol. **75**, 814–825.

Weinberg, H., and Keenan, R. (**1996**). "Gaussian ray bundles for modeling high-frequency propagation loss under shallow-water conditions," J. Acoust. Soc. Am. **100**, 1421–1431.

Wiggins, S. M., McDonald, M. A., and Hildebrand, J. A. (**2012**). "Beaked whale and dolphin tracking using a multichannel autonomous acoustic recorder," J. Acoust. Soc. Am. **131**, 156–163.

Zimmer, W. M. X., Harwood, J., Tyack, P., Johnson, M., and Madsen, P. (**2008**). "Passive acoustic detection of deep-diving beaked whales," J. Acoust. Soc. Am. **124**, 2823–2832.

Zimmer, W. M. X., Johnson, M. P., D'Amico, A., and Tyack, P. L. (**2003**). "Combining data from a multisensor tag and passive sonar to determine the diving behavior of a sperm whale (*Physeter macrocephalus*)," IEEE J. Oceanic Eng. **28**, 13–28.

Zimmer, W. M. X., Johnson, M. P., Madsen, P. T., and Tyack, P. L. (**2005**). "Echolocation clicks of free-ranging Cuvier's beaked whales (*Ziphius cavirostris*)," J. Acoust. Soc. Am. **117**, 3919–3927.